A Real-time Tool for Human Ergonomics Assessment based on Joint Compressive Forces

Luca Fortini[1,2*], Marta Lorenzini[1,2*], Wansoo Kim[1], Elena De Momi[2], and Arash Ajoudani[1]

***Abstract*— The objective of this paper is to present a mathematical tool for real-time tracking of whole-body compressive forces induced by external physical solicitations. This tool extends and enriches our recently introduced ergonomics monitoring system to asses the level of risk associated with human physical activities in human-robot collaboration contexts. The methods developed so far only considered the effect of the external loads on joint torque variations. However, even for negligible values of the joint torque overloadings (e.g., in singular configurations), the effect of compressive forces, defined by the internal/pushing forces among body links, can be significant. Accordingly, we propose the joint compressive forces as an additional real-time index for the assessment of human ergonomics. First, a simulation study is performed to validate the method. Then, follows a laboratory study on five subjects to compare the trend of the joint compressive forces with muscle activities. Results demonstrate the significance of the proposed index in the development of a comprehensive human ergonomics monitoring framework. Based on such a framework, robotic strategies as well as feedback interfaces can be employed to guide and optimise the human movement toward more convenient body configurations thus avoiding pain and consequent injuries.**

I. Introduction

According to the recent strategics [1] and scientific [2] reports, human-robot collaboration (HRC) will become a standard industry practice in the near future. Without a doubt, over the past decade, robotics, control, human modeling and anticipation tools have seen incredible signs of progress in this field, with the aim to create safe and efficient hybrid workplaces. In this direction, the benefits that would arise from the workplace personalisation aimed at improving comfort and ergonomics would be countless, not only in increasing the overall productivity, but also in enhancing the quality of life of human workers. Nevertheless, for the time being, the available tools to assess human ergonomics are not flexible enough to match the requirements of a dynamically varying work environment [3]. This issue has triggered fresh demands for the creation of a flexible and real-time ergonomics monitoring system to make humans aware of the level of risks associated with their activities. Such a system would be thereby employed to guide their movements toward more convenient body configurations, using robotic strategies [4] or feedback modalities [5], to ensure healthy working conditions.

[1]Human-Robot Interfaces and physical Interaction Laboratory, Istituto Italiano di Tecnologia, Genoa, Italy, Email: luca.fortini@iit.it

[2]Department of Electronics, Information and Bioengineering, Politecnico di Milano, Milano, Italy.

[*]Contributed equally to the work.

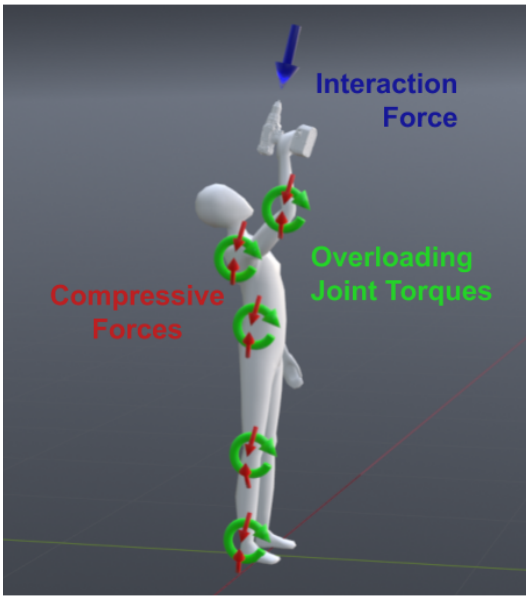

Fig. 1: Explanatory body posture in which interaction force profiles (magnitude and direction) may result in small joint torques due to a small lever arm. This may lead to a wrong pose assessment mistaking it for a healthy working condition. However, these can induce high compressive forces at body joints, increasing the risk of work-related musculoskeletal disorders.

The first step towards addressing the above specifics is the development of a set of real-time computable indexes which account for the different ergonomic risk factors [6], [7]. Accordingly, a human model was recently presented in [8], which is based on a pre-identified statically equivalent serial chain (SESC) scheme [9], and on the variations of the centre of pressure (CoP) and the vertical ground reaction force (vGRF) to compute the induced effect of external loads on body joint torques. This real-time index, called "overloading joint torque", was developed to alert humans about excessive physical stress and consequent injuries. Then, the cumulative effect of the overloading joint torque in prolonged activities was studied in [10], under a new index called the "overloading fatigue".

Although these indexes provide a good estimation of the loading effect of the external forces on body joints (acting as overloading torques), they neglect another equally important aspect, i.e., the application of balanced inward ("pushing") forces known as the compressive forces. This is an important index, since in certain configurations and external force profiles (e.g., see Fig. 1), even if the overloading joint torques are small in some joints, the compressive forces can be high

that pose risks to human health. In addition, our previous models computed the overloading torques based on objects' gravitational loads, and not on the interaction forces' arbitrary directions in task space. The objective of this paper is to address these issues by introducing a new mathematical tool for the real-time estimation of the whole-body compressive forces. The new model is also conceived for including in the computation arbitrary task interaction forces directions in the task space. First, a simulation study is provided to demonstrate the importance of the compressive forces in the assessment of human ergonomics. Next, the experimental results on five subjects performing a manipulation task are discussed, where we include an electromyography (EMG) analysis to confirm the validity of the proposed method.

The rest of the paper is organized as follows. In Sec. II a method to estimate the compressive forces is presented. Sec. III provides an experimental validation of the method, both in simulation and laboratory settings. Finally, in Sec. IV, we discuss the results and highlight future plans.

II. Method Overview

As mentioned in Sec. I, this work aims at adding a new real-time index to the observation layer of a more sophisticated human ergonomics framework (see Fig. 2), whose multi-layer approach is based on our previous works [4], [10]. The methods developed so far, of which a brief summary is provided hereafter, only considered the effect of the external loads on joint torque variations, neglecting the internal forces among body links and thus motivating the introduction of the new index. The overloading joint torques are estimated based on the displacement of the human CoP, obtained from the difference between an estimated one, $\hat{\mathbf{C}}_{P_{wo}}$, and a measured one, $\mathbf{C}_{P_{wt}}$, recorded using a suitable sensor device. Accordingly, the overloading joint torque vector can be computed as

$$\Delta\tau_s = \mathbf{S}^T \left(\tau_{wt} - \tau_{wo}\right), \tag{1}$$

where $\mathbf{S} = [\mathbf{0}_{n\times 6} \quad \mathbf{I}_{n\times n}] \in \mathbb{R}^{n\times(n+6)}$ is the actuation matrix with n the number of human body joints, and $\tau_{\text{wo}} \in \mathbb{R}^n$ and $\tau_{\text{wt}} \in \mathbb{R}^n$ are, respectively, the vectors of the torque induced on the joints in unloaded (no interaction with the environment except the ground) and loaded (interaction with i.e., a tool or a weight) conditions, while maintaining balance on quasi-static movements. Considering $\mathbf{f}_{wo}$ and $\mathbf{f}_{wt}$ as the vGRF vectors applied at the CoP without and with the effect of external forces and $\mathbf{f}_h$ as the interaction force vectors that are applied at the contact points $\mathbf{a}_h$, such quantities can be respectively computed as

$$\mathbf{S}^T\boldsymbol{\tau}_{wo} = \boldsymbol{\tau}_b - \sum_{l=1}^{n_f} \mathbf{J}^T_{\hat{C}_{P_{wo}l}} \mathbf{f}_{wo,l}. \tag{2}$$

$$\mathbf{S}^T\boldsymbol{\tau}_{wt} = \boldsymbol{\tau}_b - \sum_{l=1}^{n_f} \mathbf{J}^T_{C_{P_{wt}l}} \mathbf{f}_{wt,l} - \sum_{j=1}^{n_h} \mathbf{J}^T_{a_hj} \mathbf{f}_{h,j}, \tag{3}$$

where $\boldsymbol{\tau}_b = \mathbf{M}\ddot{\mathbf{q}} + \mathbf{C}\dot{\mathbf{q}} + \mathbf{G} \in \mathbb{R}^{n+6}$, $\mathbf{M}$, $\mathbf{C}$ and $\mathbf{G}$ represent the inertia matrix, the vector of centrifugal and Coriolis forces, and the vector of the gravity force, respectively. n_f is the number of contact forces exchanged with the ground and n_h is the number of contact points where the external forces are applied. $\mathbf{J}_{p_k}$ is the contact Jacobian at the point $\mathbf{p}_k$ with respect to the inertial reference frame Σ_W (i.e. the CoP or the interaction forces application points $\mathbf{a}_h$). The method just described is based on the modelling of the human as a floating base kinematic chain. The pelvis reference frame is set as the base frame Σ_0 attached to the inertial frame Σ_W through six virtual degrees of freedom (DoFs). The generalized coordinate of the system is defined by $\mathbf{q} = \begin{bmatrix}\mathbf{x}_0^T & \theta_0^T & \mathbf{q}_h^T\end{bmatrix}^T \in \mathbb{R}^{6+n}$. $\mathbf{x}_0^T$ and θ_0^T represent the position and the orientation of the base frame Σ_0, respectively. $\mathbf{q}_h \in \mathbb{R}^n$ denotes the angular position of human joints. Each joint reference frame, with joint index $i \in [1 \quad \cdots \quad n]$, can be denoted by Σ_i. Basically, τ_{wo} and τ_{wt} should be equal if no interactions of the human with the environment (or with an object) are in place while, in the contrary case, τ_{wo} and τ_{wt} differ and the overloading joint torque vector $\Delta\tau_s$ is able to convey the physical load exerted on the human's joints. The overloading joint torque

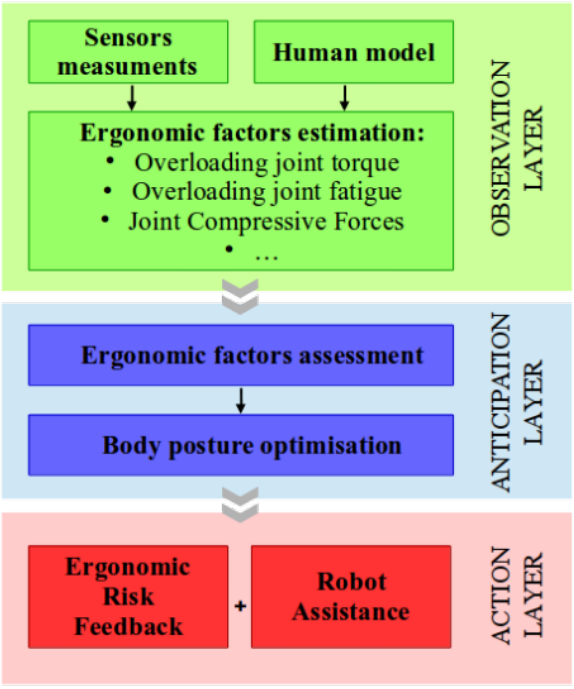

Fig. 2: The overall framework for human ergonomics monitoring and improvement in HRC scenarios. The first step consists in collecting the measurements of the human movement and of the forces the human exchange with the external environment and defining a human model to be fed with these data. Then, a set of indexes which address different ergonomic risk factors (mechanical joint overloading, movements repetitiveness, etc.) is developed to provide a comprehensive human ergonomics monitoring system (OBSERVATION). Next, by assessing the set of indexes an optimisation procedure is performed to obtain the human body configuration which minimise the ergonomic risk factors addressed (ANTICIPATION). Lastly, the human can be guided toward the optimised postures, either following a feedback provided by a visual interface/vibro-tactile devices or with assistance of a colaborative robot (ACTION).

index is hence highly dependent on the contact Jacobian of the interaction forces as well as their orientations. As a matter of fact, there are several combinations of postures and task-dependent forces profiles (magnitude and direction) that lead to a not significant CoP displacement and thus may result in the underestimation of the ergonomic factor. A scenario like the one depicted in Fig. 1 fall in the just mentioned cases, namely, body configurations at the limit of the human reachability map and interaction forces with low lever arm but high compressive potential on the joints. Accordingly, an additional index which covers the just mentioned conditions needs to be integrated in the framework.

Inverse dynamics methods applied to detailed biomechanics models may give an accurate estimate of what is going on at the joint level. However, the high computational cost is detrimental to real-time applications [11]. On the other hand, a simpler free-body diagram approach is therefore preferable, which takes into account the only effect of the external forces applied at the upper limb's endpoints on the body joints and links, in accordance with Newton's third law. Accordingly, the effect of an external force $\mathbf{f}_h$ on the body joint i can be calculated by

$$\mathbf{f}_{h,i} = \mathbf{R}_0^i \mathbf{R}_W^0 \mathbf{f}_h, \tag{4}$$

where $\mathbf{R}_i^0$ express the orientation of frame Σ_0 relative to frame Σ_i and $\mathbf{R}_W^0$ express the orientation of frame Σ_W relative to frame Σ_0. Both these rotation matrices for all the DoF can be derived from the joint angles $\mathbf{q}_h$ collected by means of a motion-capture system. The whole procedure is considered in quasi-static conditions, moreover, the gravitational effects due to the body-subject inertial parameters do not affect the calculation in any configuration. It must be cleared that there is no intention in calculating biomechanics related quantities. The forces obtained from (4), which from now on will be referred as joint compressive forces, are the result of geometric considerations and can be regarded as an additional index to evaluate human ergonomics.

For both the overloading joint torque vector $\Delta\tau_s$ and the joint compressive force vector $\mathbf{f}_{h,i}$, some specific levels can be established to render their interpretation easier and their reading more straightforward. Accordingly, we define three ergonomics index levels as illustrated in Table I. Considering $|\omega_i|$ as an ergonomics index's current absolute value and $\omega_{\max_i}$ as its maximum value, such a progressive scheme can be likewise employed for the overloading joint vector $\Delta\tau_s$ and for the joint compressive force vector $\mathbf{f}_{h,i}$.

The tuning of the maximum values was performed experimentally eliciting the joints with increasing load profiles one at a time until discomfort was manifested by the subject. The resulting values were then compared with those found in literature [12].

TABLE I: Step-wise scheme for ergonomics index levels.

Ergonomics index level	Control threshold
LOW	$0 < \lvert\omega_i\rvert \leq 0.3\ \omega_{\max_i}$
MEDIUM	$0.3\ \omega_{\max_i} < \lvert\omega_i\rvert \leq 0.6\ \omega_{\max_i}$
HIGH	$0.6\ \omega_{\max_i} < \lvert\omega_i\rvert \leq \omega_{\max_i}$

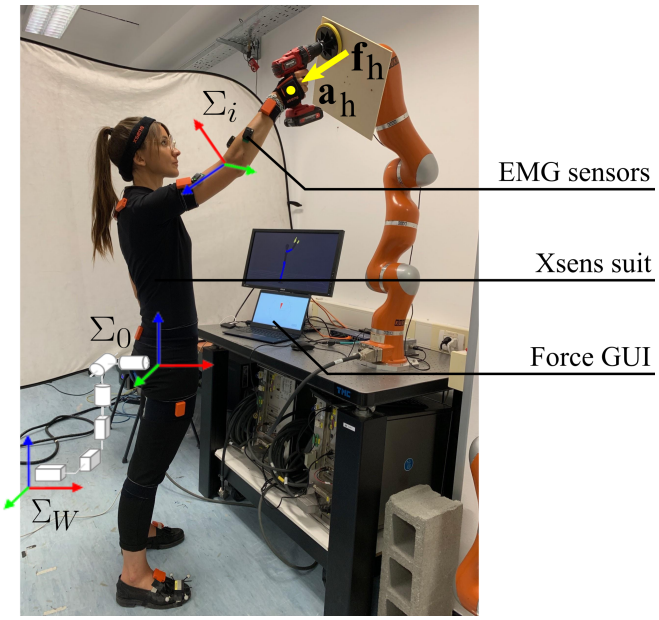

Fig. 3: Experimental setup of the laboratory experiments on five subjects. The pelvis reference frame is set as the base frame Σ_0 attached to the inertial frame Σ_W through six virtual DoFs. Σ_i is the reference frame of the i-th link. The yellow arrow represents the external force f_h applied on the human body at the contact point a_h.

III. Experimental Analysis

In this section, an experimental analysis is presented to validate the proposed ergonomics index. First, a simulation study is performed with Simscape Multibody™ (formerly SimMechanics™), a multibody simulation environment for 3D mechanical systems. Two different comparisons are made: between the joint compressive forces and the overloading joint torques and among joint compressive forces induced by different external forces. The outcome highlights how the estimation of overloading joint torques in some cases fails to detect awkward body configurations while the joint compressive forces exhibit considerable values and thus indicate a risky condition. The other way around is demonstrated as well in the same experiment. Next, a laboratory study is carried out on five participants to investigate the trend of joint compressive forces in comparison to human muscular activity. The whole experimental procedure was approved by the ethics committee Azienda Sanitaria Locale Genovese (ASL) N.3 (Protocol IIT_HRII_001).

A. Experimental setup

In the simulation study, 5 body configurations were simulated considering a 5-links simplified human body model. In each configuration, an external force was applied on the human body, equal to a vertical force (the only non-zero component was the vertical one) exerted on the hand, with a view to simulating the weight of an object held by the human. The simulation was run twice, using an external force equal to 10 N and 20 N, respectively. In each condition, the human CoP and vGRF were simulated to estimate the overloading joint torque vector $\Delta\tau_s$ according to (1) and the joint compressive force vector $\mathbf{f}_{h,i}$ was computed using (4).

For the laboratory experiments, 5 healthy volunteers, 2 females and 3 males, (age: 28.2 ± 2.9 years; mass: 65.2 ± 9.8 kg; height: 172.6 ± 5.0 cm) were recruited. After explaining the experimental procedure, a written informed consent was obtained. The experimental setup of the subject study is shown in Fig. 3. Each subject was asked to wear a MVN Biomech suit (Xsens Tech) provided with 17 inter-connected inertial measurement unit (IMU) sensors to record the whole-body motion. A graphic user interface (GUI) was provided to the subjects showing the intensity of the force exerted on the board throughout the task. This way it was possible to uniform the procedure across the subjects for a coherent comparison. Additionally, 8 electromyography (EMG) surface electrodes (Trigno Platform by Delsys) were placed on the subjects' bodies to detect the muscle activity, specifically on the following muscles: Flexor Carpi (FC), Extensor Carpi (EC), Biceps Brachii (BB), Triceps Brachii (TB), Anterior Deltoid (AD), Posterior Deltoid (PD) Latissimus Dorsi (LD) and Lumbar Erector Spinae (ES). It should be noted that the selected muscles belong mostly to the human arm and torso, which were the most involved human body parts for the task considered in this paper. Prior to the experiments, the maximal voluntary contraction (MVC) for each muscle was extracted for the subsequent normalisation of EMG data. Each subject was asked to carry out one experimental session with the request to perform a polishing task on a board using a 2.5 kg polisher. The board was provided with a force/torque (F/T) sensor to detect the interaction force between the tool and the working piece. The opposite of such a force was considered as the external force induced on the human end-effector (i.e., the right hand). It should be noted that, while in the simulation study a purely vertical external force was considered, all the components of the external force vector are non-zero in the experimental analysis. During each experimental session, the board was placed in 4 different positions and with different orientations in the workspace. Hence, each subject was required to adopt 4 different body postures and perform the polishing task in each experimental configurations for 10 seconds exerting a constant force of 20N. The subjects were asked to limit their movements along the sagittal plane since a human sagittal model is considered in this paper. The data regarding the human whole-body motion, the force exerted on the working piece as well as the human muscle activity were recorded throughout all the experimental sessions. Based on them, the joint compressive force vector $\mathbf{f}_{h,i}$ was computed using (4) and the percentage of the MVC was obtained for each subject. The different sensor devices were interconnected and integrated through the Robot Operating System (ROS) environment.

B. Results and discussion

The results of the simulation study are presented in Fig. 4 and Fig. 5. In Fig. 4, the 2 most emblematic body configurations are considered to show the different risk factors addressed by the overloading joint torques and the joint compressive forces. Such body configurations are illustrated through a 2-D stick-model of the human in the left graphs.

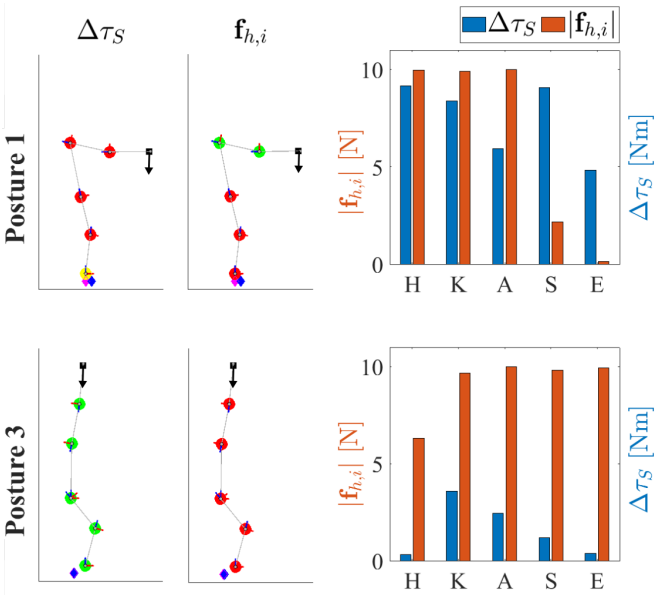

Fig. 4: Results of the simulation study for 2 body configurations. The human body configurations represented through 2-D stick-models with superimposed spheres displaying the overloading torque vector $\Delta\tau_s$ (first column) and the compressive force vector $\mathbf{f}_{h,i}$ (second column) color-coded to denote the level of the corresponding index, according to Table I, are illustrated in the left graphs. The absolute values of such quantities are represented in the right graphs for the most significant human joints: hip (H), knee (K), ankle (A), shoulder (S) and elbow (E).

The overloading torque vector $\Delta\tau_s$ and the compressive force vector $\mathbf{f}_{h,i}$ induced on the human joints by an external force equal to 10 N (illustrated by a black arrow) are displayed through spheres superimposed on the stick-model, in the first column, and in the second column, respectively. The spheres are color-coded to denote a high (red), medium (yellow) or (low) level of the corresponding ergonomics index. The 3 levels are determined as explained in Table I, Sec. II. Additionally, the absolute values of such quantities are represented in the right graphs for the most significant human joints: hip (H), knee (K), ankle (A), shoulder (S) and elbow (E). In posture 1 (first row of the figure), the external force is transversal to the imaginary line formed by the human arm thus it induces high overloading joint torques but low joint compressive forces. On the contrary, in posture 3 (second row of the figure), the external force is longitudinal to the human arm line thus it entails the opposite effect: low overloading joint torques but high joint compressive forces. Based on the latter considerations, it is evident that the integration of the overloading joint torques with the joint compressive forces is required to establish a comprehensive system to evaluate human ergonomics. In fact, to identify all the conceivable risky conditions for the human, both the variations of the external force exerted on the body and its different effects on the body structure must be considered.

In Fig. 5 all the 5 body configurations are illustrated through the 2-D stick-model of the human in the first row of the figure, with a black arrow displaying the external force applied on the human body. In the second row, a graph is presented for each body configuration, which shows the

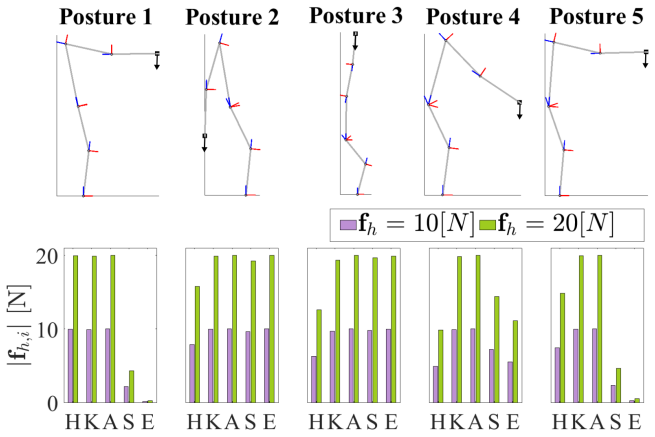

Fig. 5: Results of the simulation study for all the 5 body configurations. The body configurations are illustrated through a 2-D stick-model of the human in the first row. The absolute values of the compressive force vector $|\mathbf{f}_{h,i}|$ induced on the most significant human joints (hip (H), knee (K), ankle (A), shoulder (S) and elbow (E)) by an external force equal to 10 N and 20 N, respectively, are represented in the second row.

absolute values of the compressive force vector $|\mathbf{f}_{h,i}|$ induced on the most significant human joints by an external force equal to 10 N and 20 N, respectively. It can be noted how, by maintaining the force vector orientation but changing its module, the joint compressive forces increase proportionally. However, the important aspect to underline is the sensitivity of the joint compressive forces to the external force vector variations.

The results of the laboratory experiments are presented in Fig. 6 for one subjects (subject 2). In the first row of the figure, all the 4 body configurations are depicted through the 2-D stick-model of the human. The compressive force vector $\mathbf{f}_{h,i}$ induced on the human joints by the external force (illustrated by a black arrow) is displayed through spheres superimposed on the stick-model and color-coded to denote the level of the ergonomics index, according to Table I, Sec. II. Additionally, in the last row of the figure, the absolute values of the compressive forces in the most significant human joints are presented for each body configuration. A 9 DoF human model is considered which includes: hip (H), knee (K), ankle (A), 5^{th} lumbar vertebrae (L5), 3^{rd} lumbar vertebrae (L3), 12^{th} thoracic vertebrae (T12), 8^{th} thoracic vertebrae (T8), shoulder (S) and elbow (E). Multiple DoF are taken into account for the human spine since it proves to be the more affected body part by the compressive forces. The colored bars represent the average while the black lines represent the standard deviations of the compressive forces computed over the duration (10 seconds) of the polishing task in each posture. Finally, in the second row of the figure, the percentages of the MVC of all the analysed muscles are presented for each body configuration. Similarly to the compressive forces graphs, the colored bars represent the average while the black lines represent the standard deviations of the % MVC computed over the duration of the task in each posture. The outcomes for all the other subjects are presented individually in Table II. The compressive forces in L5, L3, T12, and T8 have been here averaged and summarised in one joint since they had similar values. On the other hand, in Fig. 7 the inter-subjects results are presented. In the first row of the figure, the mean and the standard deviation of the percentages of the MVC of all the analysed muscles computed among all the subjects for each body configuration are provided. Similarly, in the second row, the mean and the standard deviation of the absolute values of the compressive forces in the main human joints computed among all the subjects for each body configuration are shown.

Althought the external force repartition over the joints cannot be directly related to physiological quantities as muscle activity, it can be seen that, in general, lower compressive forces correspond to minor muscle activity. Observing Fig. 6 and 7 and focusing on the compressive forces induced in the shoulder and in the elbow, which are the most involved body parts in the task analysed in this paper, it can be noted that in posture 1 and 3 they present higher values than in posture 2 and 4. Correspondingly, the percentage of the MVC of all the analysed muscles is generally higher in posture 1 and 3 than in posture 2 and 4.

Accordingly, we can state that the proposed ergonomics index shows promising capabilities to detect body configurations which are awkward and risky for humans.

IV. Conclusion

In this paper, we introduced an index to monitor the compressive forces induced on the human joints by external physical interactions. The proposed method has been proven to be an effective tool in assessing the ergonomics of humans during dynamic interactions with the environment. The proposed index extends and complements our previously developed ergonomics monitoring framework which was based on the overloading torque and fatigue estimation.

Our final objective is to establish a comprehensive system for the real-time assessment of human ergonomics that account for different risk factors in the workplace. This will be achieved by integrating all the ergonomics assessment tools that we have proposed so far into a unified system.

V. Acknowledgements

This work was supported by the European Research Council (ERC) starting grant Ergo-Lean, Grant Agreement No. 850932.

References

[1] B. Vanderborght, "Unlocking the potential of industrial human–robot collaboration," European Commission, Directorate-General for Research and Innovation, Tech. Rep., 2019.

[2] A. Ajoudani, A. M. Zanchettin, S. Ivaldi, A. Albu-Schäffer, K. Kosuge, and O. Khatib, "Progress and prospects of the human–robot collaboration," *Autonomous Robots*, vol. 42, no. 5, pp. 957–975, 2018.

[3] G. Li and P. Buckle, "Current techniques for assessing physical exposure to work-related musculoskeletal risks, with emphasis on posture-based methods," *Ergonomics*, vol. 42, no. 5, pp. 674–695, 1999.

[4] W. Kim, J. Lee, L. Peternel, N. Tsagarakis, and A. Ajoudani, "Anticipatory robot assistance for the prevention of human static joint overloading in human–robot collaboration," *IEEE robotics and automation letters*, vol. 3, no. 1, pp. 68–75, 2017.

TABLE II: Results of the laboratory experiments for all the subjects. The mean and the standard deviation of the percentages of the MVC of all the analysed muscles and the mean and the standard deviation of the absolute values of the compressive force vector $|\mathbf{f}_{h,i}|$ in the most significant human joints, are presented for each subject.

Subject 1

	Joint Compressive Forces $\|\mathbf{f}_{h,i}\|$ [N]						% MVC							
Posture	H	K	A	Spine	S	E	ES	LD	PD	AD	TB	BB	EC	FC
1	9.8 ± 2.1	11.3 ± 2.3	9.3 ± 2.0	8.6 ± 1.9	14.5 ± 2.6	17.1 ± 3.1	13.7 ± 2.8	27.0 ± 4.6	38.0 ± 4.6	27.8 ± 3.6	37.9 ± 3.3	13.8 ± 1.4	12.8 ± 2.0	27.0 ± 2.3
2	7.5 ± 3.5	8.1 ± 3.7	7.1 ± 3.3	10.2 ± 4.8	10.4 ± 5.0	11.2 ± 5.1	17.8 ± 2.8	13.5 ± 1.5	4.0 ± 1.7	2.6 ± 0.4	58.3 ± 16.9	5.8 ± 0.6	15.5 ± 4.0	6.0 ± 2.2
3	3.8 ± 1.2	5.6 ± 1.5	2.9 ± 1.0	3.2 ± 1.0	13.3 ± 2.9	17.4 ± 3.7	13.0 ± 2.9	27.4 ± 4.7	24.2 ± 1.9	14.6 ± 1.5	26.9 ± 1.6	9.2 ± 1.2	11.6 ± 1.4	34.6 ± 4.3
4	1.6 ± 0.9	2.7 ± 1.2	1.0 ± 0.6	4.5 ± 1.7	5.9 ± 2.1	17.9 ± 5.0	15.7 ± 2.6	12.3 ± 1.6	1.9 ± 0.1	2.4 ± 0.1	38.9 ± 4.3	6.0 ± 0.4	21.5 ± 10.0	18.2 ± 7.2

Subject 3

	Joint Compressive Forces $\|\mathbf{f}_{h,i}\|$ [N]						% MVC							
Posture	H	K	A	Spine	S	E	ES	LD	PD	AD	TB	BB	EC	FC
1	7.8 ± 2.1	8.1 ± 2.2	6.4 ± 1.7	7.1 ± 1.9	13.3 ± 3.4	17.8 ± 4.9	10.7 ± 1.7	11.3 ± 0.9	47.3 ± 4.0	12.5 ± 1.0	6.5 ± 1.5	11.9 ± 0.9	1.2 ± 0.5	11.2 ± 1.3
2	6.7 ± 2.2	7.0 ± 2.3	5.8 ± 1.9	10.3 ± 3.6	10.1 ± 3.5	12.0 ± 4.8	28.2 ± 2.7	9.6 ± 1.8	1.7 ± 0.5	0.6 ± 0.1	10.7 ± 1.7	3.9 ± 0.3	2.0 ± 0.5	15.3 ± 2.4
3	2.9 ± 1.4	4.5 ± 1.7	2.4 ± 0.9	2.0 ± 1.2	11.5 ± 3.7	16.8 ± 5.1	16.2 ± 6.9	10.8 ± 1.4	28.2 ± 8.1	4.3 ± 2.0	6.8 ± 3.5	7.2 ± 1.7	2.2 ± 2.0	13.2 ± 3.0
4	1.5 ± 0.6	2.4 ± 0.9	1.2 ± 0.5	4.0 ± 1.4	5.2 ± 1.8	16.8 ± 5.2	19.2 ± 2.0	9.9 ± 3.9	1.4 ± 0.2	0.6 ± 0.1	10.1 ± 1.3	4.2 ± 0.3	2.7 ± 2.3	13.0 ± 1.3

Subject 4

	Joint Compressive Forces $\|\mathbf{f}_{h,i}\|$ [N]						% MVC							
Posture	H	K	A	Spine	S	E	ES	LD	PD	AD	TB	BB	EC	FC
1	7.7 ± 1.6	8.8 ± 1.9	6.9 ± 1.4	5.8 ± 1.2	16.6 ± 4.2	17.8 ± 4.2	12.6 ± 1.3	47.9 ± 5.0	72.6 ± 10.8	13.1 ± 1.9	14.2 ± 4.1	20.3 ± 1.2	47.6 ± 6.9	17.9 ± 1.8
2	8.2 ± 2.3	8.8 ± 2.4	6.9 ± 1.9	8.5 ± 2.4	6.5 ± 1.8	14.5 ± 3.8	10.8 ± 2.3	26.5 ± 3.4	24.3 ± 7.4	1.7 ± 0.3	40.7 ± 6.4	8.5 ± 0.7	1.0 ± 0.1	11.2 ± 1.2
3	3.2 ± 0.8	4.0 ± 1.0	1.7 ± 0.5	1.5 ± 0.5	16.8 ± 4.2	18.5 ± 4.6	17.3 ± 1.9	55.0 ± 6.5	77.9 ± 20.6	14.9 ± 2.2	22.9 ± 8.3	18.5 ± 2.2	42.4 ± 7.0	19.7 ± 2.8
4	1.0 ± 0.6	1.8 ± 0.8	0.4 ± 0.4	1.0 ± 0.6	1.1 ± 0.6	16.9 ± 4.7	4.8 ± 0.6	22.5 ± 2.9	25.2 ± 7.4	1.7 ± 0.3	32.8 ± 6.3	9.3 ± 0.9	35.0 ± 2.3	13.0 ± 1.0

Subject 5

	Joint Compressive Forces $\|\mathbf{f}_{h,i}\|$ [N]						% MVC							
Posture	H	K	A	Spine	S	E	ES	LD	PD	AD	TB	BB	EC	FC
1	1.2 ± 0.5	0.5 ± 0.4	2.5 ± 0.9	14.9 ± 3.6	6.4 ± 3.7	11.8 ± 6.6	37.7 ± 7.8	45.0 ± 6.4	56.2 ± 8.4	9.2 ± 1.2	8.1 ± 0.8	11.3 ± 1.5	5.2 ± 1.5	17.9 ± 4.8
2	0.8 ± 0.5	1.1 ± 0.5	0.7 ± 0.5	1.6 ± 1.5	12.9 ± 6.1	11.4 ± 6.2	38.8 ± 3.0	23.9 ± 1.8	11.6 ± 2.3	2.9 ± 0.2	9.9 ± 1.6	8.4 ± 0.8	4.2 ± 1.8	38.5 ± 2.2
3	4.3 ± 1.4	4.7 ± 1.4	3.1 ± 1.2	3.9 ± 1.2	13.9 ± 5.6	12.8 ± 6.6	64.2 ± 9.3	43.2 ± 6.1	54.6 ± 3.4	9.2 ± 1.2	6.7 ± 1.3	17.1 ± 2.3	3.4 ± 0.6	26.0 ± 4.8
4	11.1 ± 6.6	5.8 ± 2.5	1.1 ± 0.5	3.9 ± 2.1	13.9 ± 4.5	15.3 ± 4.6	42.5 ± 3.0	25.7 ± 3.0	16.4 ± 2.4	3.1 ± 0.2	6.3 ± 1.2	7.0 ± 0.7	6.1 ± 2.1	26.3 ± 3.8

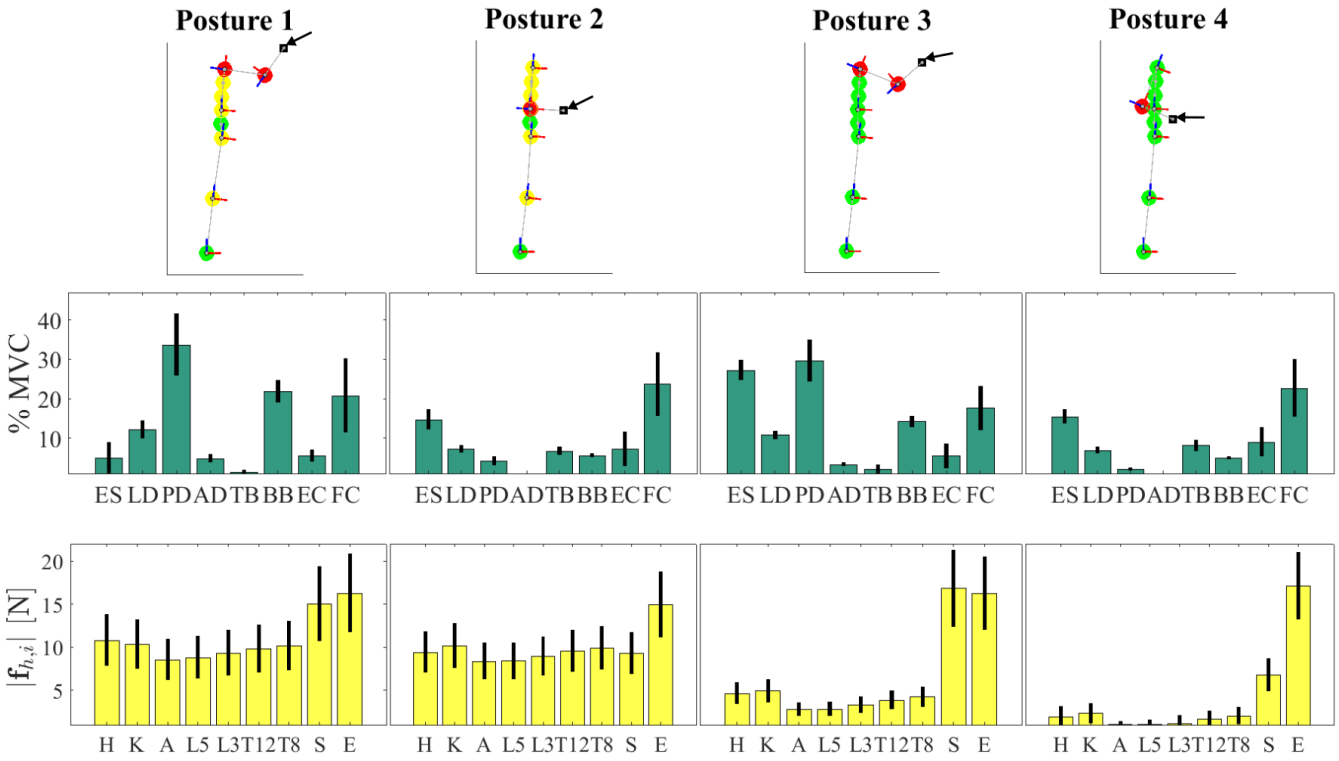

Fig. 6: Results of the laboratory experiments for one subject. The human body configurations represented through 2-D stick-models with superimposed spheres displaying the compressive force vector $\mathbf{f}_{h,i}$ color-coded to denote the level of the index, according to Table I, are illustrated in the first row. The mean and the standard deviation of the percentages of the MVC of all the analysed muscles (Flexor Carpi (FC), Extensor Carpi (EC), Biceps Brachii (BB), Triceps Brachii (TB), Anterior Deltoid (AD), Posterior Deltoid (PD) Latissimus Dorsi (LD) and Lumbar Erector Spinae (ES)) computed over the duration of the polishing task for each body configuration are presented in the second row. The mean and the standard deviation of the absolute values of the compressive force vector $|\mathbf{f}_{h,i}|$ in the most significant human joints (hip (H), knee (K), ankle (A), 5^{th} lumbar vertebrae (L5), 3^{rd} lumbar vertebrae (L3), 12^{th} thoracic vertebrae (T12), 8^{th} thoracic vertebrae (T8), shoulder (S) and elbow (E)) computed over the duration of the polishing task for each body configuration are presented in the third row.

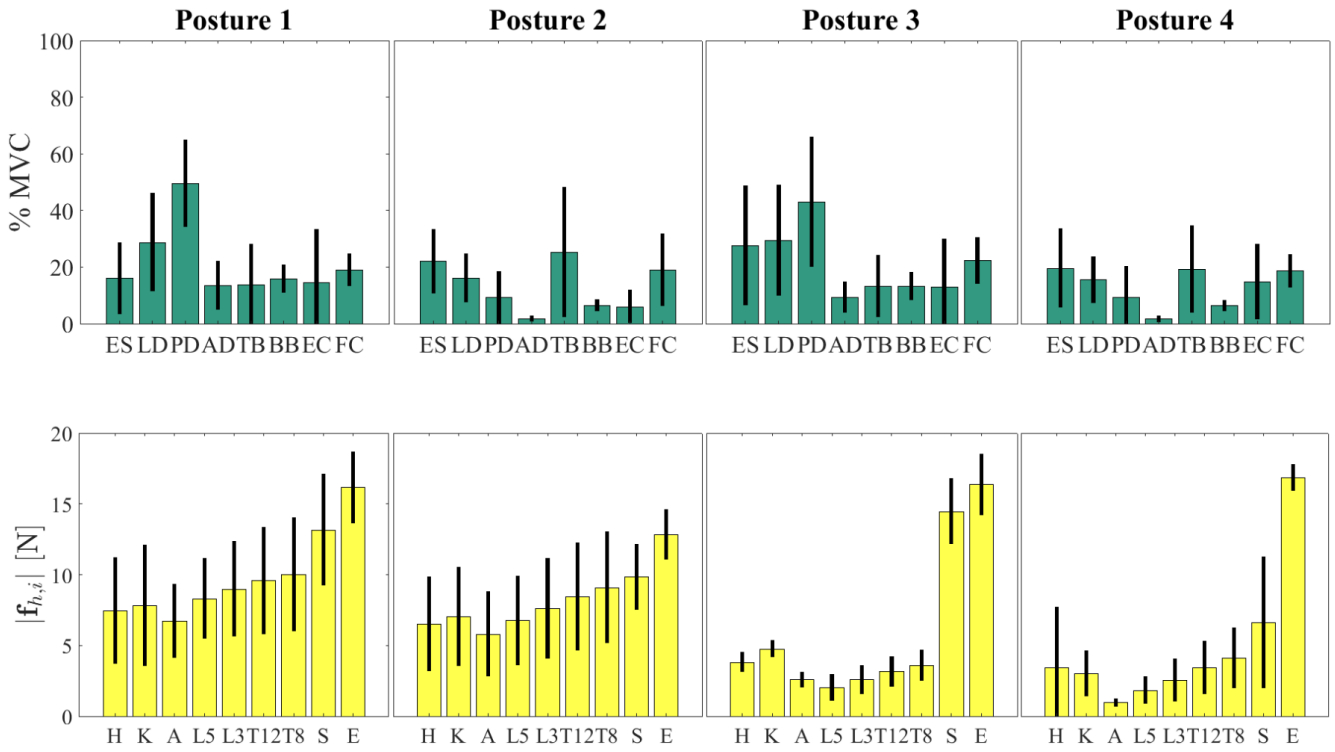

Fig. 7: Results of the inter-subject analysis. The mean and the standard deviation of the percentages of the MVC of all the analysed muscles computed among all the subjects for each body configuration are presented in the first row. The mean and the standard deviation of the absolute values of the compressive force vector $|\mathbf{f}_{h,i}|$ in the most significant human joints computed among all the subjects for each body configuration are presented in the second row.

[5] S. Casini, M. Morvidoni, M. Bianchi, M. Catalano, G. Grioli, and A. Bicchi, "Design and realization of the cuff-clenching upper-limb force feedback wearable device for distributed mechano-tactile stimulation of normal and tangential skin forces," in *2015 IEEE/RSJ International Conference on Intelligent Robots and Systems (IROS)*. IEEE, 2015, pp. 1186–1193.

[6] A. Malaisé, P. Maurice, F. Colas, and S. Ivaldi, "Activity recognition for ergonomics assessment of industrial tasks with automatic feature selection," *IEEE Robotics and Automation Letters*, vol. 4, no. 2, pp. 1132–1139, 2019.

[7] W. Kim, M. Lorenzini, P. Balatti, P. D. Nguyen, U. Pattacini, V. Tikhanoff, L. Peternel, C. Fantacci, L. Natale, G. Metta *et al.*, "Adaptable workstations for human-robot collaboration: A reconfigurable framework for improving worker ergonomics and productivity," *IEEE Robotics & Automation Magazine*, vol. 26, no. 3, pp. 14–26, 2019.

[8] W. Kim, J. Lee, N. Tsagarakis, and A. Ajoudani, "A real-time and reduced-complexity approach to the detection and monitoring of static joint overloading in humans," in *2017 International Conference on Rehabilitation Robotics (ICORR)*. IEEE, 2017, pp. 828–834.

[9] S. Cotton, A. P. Murray, and P. Fraisse, "Estimation of the center of mass: from humanoid robots to human beings," *IEEE/ASME Transactions on Mechatronics*, vol. 14, no. 6, pp. 707–712, 2009.

[10] M. Lorenzini, W. Kim, E. De Momi, and A. Ajoudani, "A new overloading fatigue model for ergonomic risk assessment with application to human-robot collaboration," in *2019 International Conference on Robotics and Automation (ICRA)*. IEEE, 2019, pp. 1962–1968.

[11] R. W. Bisseling and A. L. Hof, "Handling of impact forces in inverse dynamics," *Journal of biomechanics*, vol. 39, no. 13, pp. 2438–2444, 2006.

[12] S. H. Snook and V. M. Ciriello, "The design of manual handling tasks: revised tables of maximum acceptable weights and forces," *Ergonomics*, vol. 34, no. 9, pp. 1197–1213, 1991.